



Contents lists available at ScienceDirect

## Saudi Journal of Biological Sciences

journal homepage: [www.sciencedirect.com](http://www.sciencedirect.com)

Original article



## *In vitro* and *in silico* studies of the potential cytotoxic, antioxidant, and HMG CoA reductase inhibitory effects of chitin from Indonesia mangrove crab (*Scylla serrata*) shells

Inarah Fajriaty<sup>a,c,\*</sup>, Irda Fidrianny<sup>b</sup>, Neng Fisher Kurniati<sup>a</sup>, Norsyahida Mohd Fauzi<sup>d</sup>, Sarmila Hanim Mustafa<sup>d</sup>, I. Ketut Adnyana<sup>a,\*</sup>

<sup>a</sup> Department of Pharmacology and Clinical Pharmacy, School of Pharmacy, Bandung Institute of Technology, Ganesha 10, Bandung 40132, Indonesia

<sup>b</sup> Department of Pharmaceutical Biology, School of Pharmacy, Bandung Institute of Technology, Ganesha 10, Bandung 40132, Indonesia

<sup>c</sup> Department of Pharmacy, Faculty of Medicine, Universitas Tanjungpura, Hadari Nawawi, Pontianak 78124, Indonesia

<sup>d</sup> Centre for Drug and Herbal Development, Faculty of Pharmacy, Universiti Kebangsaan Malaysia, Raja Muda Abdul Aziz, Kuala Lumpur 50300, Malaysia

## ARTICLE INFO

## Keywords:

Cytotoxic  
Antioxidant  
HMG CoA reductase inhibitors  
Chitin  
In silico  
In vitro

## ABSTRACT

This study aimed to characterize chitin extracted from Indonesia mangrove crab (*Scylla serrata*) shells, as well as to assess its *in vitro* cytotoxic, antioxidant, and HMG CoA reductase inhibitory potentials. *In silico* molecular docking, molecular dynamic, and ADMET prediction analyses were also carried out. Chitin was extracted from mangrove crab shells using deproteination and demineralization processes, Scanning Electron Microscopy (SEM) and Fourier Transform Infrared (FTIR) characterization are then performed. The MTT method was further tested in a study of cell viability, while *in vitro* method was used to assess HMG CoA reductase inhibitory and antioxidant activities. The extracted chitin was found to have a moderate level of cytotoxic and antioxidant activities. *In vitro* studies showed that it has an IC<sub>50</sub> of 36,65 ± 0,082 µg/mL as an HMG CoA reductase inhibitor, and decreased enzyme activity by 68.733 % at 100 µg/mL as a concentration. Furthermore, in the *in silico* study, chitin showed a strong affinity to several targets, including HMG CoA reductase, HMG synthase, LDL receptor, PPAR-alfa, and HCAR-2 with binding energies of -5.7; -5.8; -3.6; -5.6; -4.6 kcal/mol, respectively. Based on the ADMET properties, it had non-toxic molecules, which were absorbed and distributed across the blood-brain barrier. The molecular dynamics (MD) simulation also showed that it remained stable in the active sites of HMG CoA reductase receptor for 100 ns. These results indicated that chitin from Indonesian mangrove crab shells can be used to develop more potent HMG CoA reductase inhibitor with antioxidant and cytotoxic activities for effective dyslipidemia therapy.

## 1. Introduction

Chitin compounds are found in the shells of mangrove crabs (*Scylla serrata*). Chitin content varies among different species: crabs have 60 %, shrimp 42–57 %, jellyfish 40 %, clams 14–35 %, and Hong Kong caterpillars 12.8 %. Chitin's positive benefits in the biomedical field include its use in wound healing, contact lenses, blood dialysis membranes, anticancer treatments, and cholesterol treatments and body weight reduction (Baskaran et al., 2015; Hazqil Kadzim and Hartati, 2020).

Chitin is an aminopolysaccharide polymer that is abundantly found

in the shells of crustaceans, including mangrove crab. Although the shells are often discarded as industrial waste, in the fishing industry, the constituent chitin is partially conserved as chitosan, with glucosamine acting as an intermediary (Baskaran et al., 2015; Hazqil Kadzim and Hartati, 2020; Islam et al., 2022; Ongtanasup et al., 2022; Shebis et al., 2013; Wittriansyah et al., 2018; Yunarto et al., 2019). This has led to the development of a process, where the waste is treated with an effluent purification procedure. Furthermore, the treatment helps to remove proteins and calcium carbonate residue using aqueous NaOH and HCl, thereby leading to the production of chitin (Aklog et al., 2016). This purification has been reported to increase the commercial value of the

\* Corresponding authors at: Department of Pharmacy, Faculty of Medicine, Universitas Tanjungpura, Hadari Nawawi, Pontianak 78124, Indonesia (I. Fajriaty) E-mail addresses: [inarah.fajriaty@pharm.untan.ac.id](mailto:inarah.fajriaty@pharm.untan.ac.id) (I. Fajriaty), [irda@itb.ac.id](mailto:irda@itb.ac.id) (I. Fidrianny), [nfkurniati@itb.ac.id](mailto:nfkurniati@itb.ac.id) (N.F. Kurniati), [drmorsyahida@ukm.edu.my](mailto:drmorsyahida@ukm.edu.my) (N.M. Fauzi), [P109635@siswa.ukm.edu](mailto:P109635@siswa.ukm.edu) (S.H. Mustafa), [ketut@itb.ac.id](mailto:ketut@itb.ac.id) (I.K. Adnyana).

<https://doi.org/10.1016/j.sjbs.2024.103964>

Received 17 July 2023; Received in revised form 22 February 2024; Accepted 24 February 2024

Available online 25 February 2024

1319-562X/© 2024 Published by Elsevier B.V. on behalf of King Saud University. This is an open access article under the CC BY-NC-ND license (<http://creativecommons.org/licenses/by-nc-nd/4.0/>).

product, which is now priced at around 40 USD or 600.000 IDR/kg.

Consequently, the use of natural products and their derivatives as an alternative modality in the treatment of many diseases, such as cytotoxic activity, antioxidant and antidiyslipidemia, has expanded in recent years. Natural bioactive molecules can positively impact the entire organism with reduced toxicity compared to synthetic medications. Hence, natural products are going to remain highly significant as sources for discovering new medical compounds.

Considering the vast potential of chitin as sources of antioxidant and antidiyslipidemia drugs, several studies explored the antioxidant activities of chitin, particularly those from commercial shrimp shells, which have a stronger DPPH (2,2-difenil-1-pikril-hidrazil) radical scavenging action at a concentration of 5 mg/mL. Furthermore, these materials have been reported to show similar action against the ferric ion-reducing assay (FRAP) (Ferric Reducing Antioxidant Power) (Kidibule et al., 2020). Previous investigations also revealed the existence of hypolipidemic effects from chitin derived from fungal, crustacean, and sponge sources (Al-Abbad and Alakhras, 2020; Daniar and Herdyastuti, 2019). These materials have the ability to reduce adipogenesis and the expression of genes unique to adipocytes by regulating adenosine monophosphate-activated protein kinase (AMPK) and aquaporin-7 (Kong et al., 2011). While the cytotoxic, antioxidants, and antidiyslipidemic activity of chitin from various sources have been explored, there are no *in vitro* studies on those derived from mangrove crab shells to determine their potential to inhibit HMG CoA reductase (Imtihani et al., 2021). Therefore, this is the first study to demonstrate *in vitro* cytotoxic activity, antioxidant, and anti-dyslipidemic properties of chitin from Indonesian mangrove crab shells. Additionally, a dynamic simulation and *in silico* molecular docking were carried out to predict the interactions with anti-dyslipidemic receptors, such as 3-hydroxy-3-methyl-glutaryl-coenzyme A reductase (HMG CoA reductase)(HMGR), hydroxymethylglutaryl-CoA synthase (HMG synthase), low-density lipoprotein receptor (LDL-R), peroxisome proliferator-activated receptor-alpha receptors (PPAR-alpha), and Hydroxycarboxylic Acid Receptor 2 (HCAR 2), and absorption, distribution, metabolism, and excretion-toxicity (ADMET) prediction.

## 2. Materials and methods

### 2.1. Chemicals and reagents

All reagents were purchased from Merck, and HMG CoA reductase assay kit (Catalog No. CS1090) was obtained from Sigma-Aldrich (St. Louis, USA). Human liver cancer cell line, HepG2, was obtained from NCCS, while Eagle's Minimum Essential Medium (EMEM) with 2 mM GlutaMAX (L-Glutamin) (ATCC), Fetal Bovine Serum (FBS) 10 % (Gibco, USA), and 1 % Antibiotic solution containing penicillin (100 U/mL), streptomycin (100 µg/mL) (Gibco, USA), MTT [3-(4,5-Dimethylthiazol-2-yl)-2,5-Difeniltetrazolium Bromida](Merck), FBS (Fetal Bovine Serum) 10 %, Tripsin EDTA, DMSO, Aquadest, PBS (Phospat Buffer Saline) (Gibco) were used for cell culture.

### 2.2. Collection of mangrove crab shells

Mangrove crab (*Scylla serrata*) shells were obtained from crab fisheries in Kubu Raya, West Borneo, Indonesia, and authenticated by Dr. Arni Sholihah and Mr. Ganjar Cahyadi. Subsequently, a voucher specimen was deposited in the Herbarium Bandungense, School of Life Sciences and Technology, Bandung Institute of Technology Bandung, Indonesia.

### 2.3. Extraction, characterization, and standardization of chitin from mangrove crab shells

#### 2.3.1. Deproteinization process

The dried crab shells were soaked in a 3.5 % NaOH solution with a

ratio of 1:10 and agitated during the deproteinization process. The mixture was then heated for one hour at 60–70 °C with continuous stirring at 50 rpm, followed by filtration and chilling. The precipitate was purified in distilled water until the pH level was neutral, and it was dried for 24 h at 80 °C in the oven with subsequent drying and weighing.

#### 2.3.2. Demineralization process

The product from the deproteinization stage was submerged in a 0.05 M HCl solution in a ratio of 10:1 and agitated during the demineralization stage. It was then stirred at a speed of 50 rpm with heating for one hour at 60–70 °C. Subsequently, the precipitate was dried, extracted, rinsed in distilled water until the pH level was neutral, and dried in an oven at 80 °C for 24 h. It was weighed and allowed to cool in a desiccator (Fadlaoui et al., 2019).

#### 2.3.3. Characterization, and standardization

FT-IR and SEM-EDX spectrometers were used to assess the chitin particles. The particles from mangrove crab shells were characterized and standardized using FT-IR, SEM-EDX, drying shrink, ethanol soluble level, water-soluble level, water content, total ash, acid insoluble ash, extract specific gravity (1 %), yield, melting point, ALT, *E. coli*, mold level, and yeast level. An Inductively Coupled Plasma Optical Emission Spectrometer (ICP-OES) was used to assess the level of heavy metal contamination. The molybdate vanadate method was used to analyze the chitin of mangrove crab shells to assess the metal content and heavy metal contamination (Payyappallimana and Venkatasubramanian, 2016).

### 2.4. Cell viability study of chitin from mangrove crab shells in vitro MTT assay (Microtetrazolium (3-(4,5-dimethylthiazol-2-yl)-2,5-difenil tetrazolium bromide) methods for cytotoxicity testing against HepG2 cells

#### 2.4.1. Maintenance of hepatoma cell lines for the experiment

The HepG2 liver cancer cell line was maintained using Eagle's Minimum Essential Medium (EMEM) with 2 mM GlutaMAX (L-Glutamin) supplemented with fetal bovine serum (FBS) and 1X antibiotic-antimycotic. The cell was then kept at 37 °C with 5 % CO<sub>2</sub> in a humidified atmosphere. Furthermore, to maintain the sub-confluent state, the cell was subcultured twice a week using trypsin-EDTA 0.25 % (v/v).

#### 2.4.2. Cell viability assay

The colorimetric assay 3-(4,5-dimethylthiazol-2-yl)-2, 5-diphenyltetrazolium bromide (MTT) was used to screen the activity of chitin on malignant liver cancer cell. Subsequently, the cell was seeded with Caco2 cells (1 × 10<sup>4</sup> cells/well) into 96-well plates and incubated in a CO<sub>2</sub> incubator for 24 h. The samples were then removed from the media and treated in 100 µl growth medium with a polymer solution (various concentrations and time points). The cell line was subjected to different concentrations of chitin, namely 1, 25, 50, 75, and 100 µg/mL, with further incubation for 24 h. The media was removed and replaced with 100 µl of fresh media (no serum) before performing the MTT assay. A total of 20 µl of MTT solution (5 mg/mL) was added into each well (in the dark), incubated for 4 h at 37 °C, and 100 µl of DMSO was added. The mixture was incubated for 10 min after thoroughly mixing with a pipette and a microplate reader was used to measure the absorbance (Wallac 1420 multilabel counter, PerkinElmer) at 540 nm (Nath et al., 2016).

### 2.5. In vitro antioxidant activity of chitin from mangrove crab shells

Chitin's antioxidant capacity was identified quantitatively using the DPPH and FRAP assays. In the DPPH assay, six different concentrations (1, 5, 10, 20, 40 and 80 µg/mL) of methanolic chitin solution (100 µl) were reacted with methanolic DPPH solution (1 mL, 0.4 mM) for 30 min. The absorbance was then measured by UV–vis spectrophotometer at 515 nm wavelength (Budiana et al., 2017; Wulansari et al., 2011).

Furthermore, the following formula was used for determining the percent inhibition, DPPH inhibition (%) =  $(A_0 - A_s) / A_0 \times 100$ , where  $A_0$  is the absorbance of the methanolic solution and  $A_s$  is the absorbance in the presence of the test sample. To determine the  $IC_{50}$  value, the linear regression line was drawn and the equation was obtained by plotting the DPPH inhibition (y) against the sample concentration (x) (Wulansari et al., 2011).

In the FRAP assay, six different concentrations (10, 50, 100, 200, 400 and 800  $\mu\text{g/mL}$ ) were used. The ferric-reducing ability of the plasma FRAP assay was used to calculate a sample's annual antioxidant potential. This assay was then built around a substance's reducing capability (antioxidant). The ferrous ion ( $\text{Fe}^{2+}$ ) produced a blue complex ( $\text{Fe}^{2+}/\text{TPTZ}$ ), which increased the absorbance at 593 nm when it was reduced to  $\text{Fe}^{2+}$  by a potential antioxidant. The 10:1:1 (v/v/v) mixture of acetate buffer (300 mM, pH 3.6), a solution of 10 mM TPTZ in 40 mM HCl, and 20 mM  $\text{FeCl}_3$  was used to produce the FRAP reagent. The sample solutions (100  $\mu\text{l}$ ) and reagent (3.400  $\mu\text{l}$ ) were then added to each well and thoroughly mixed, and the absorbance was measured at 593 nm after 30 min. On the day of preparation, every solution was applied, and triplicate analyses were performed on each extract.

The ultimate concentration of DPPH/FRAP was divided by the  $IC_{50}$  to determine the Antioxidant Activity Index (AAI) value. AAI values of 0.5, >0.5–1, > 1–2, and >2 indicated ineffective, moderately effective, powerful, and extremely effective antioxidants, respectively (Maesaroh et al., 2018).

## 2.6. HMG CoA reductase inhibitory test of chitin from mangrove crab shells

HMG CoA reductase assay kit (Sigma-Aldrich, Catalog No. CS1090) used in this study included pravastatin as an inhibitor, a buffer solution, NADPH, a substrate (HMG CoA), and an enzyme containing the catalytic domain of HMG CoA reductase (0.5–0.7 mg/mL-1). Sonication was carried out to dissolve 100  $\mu\text{l/mL}$  of mangrove crab shells chitin in aqua pro injection. All samples and the control inhibitor (pravastatin) were then loaded in a UV 96-well microplate with an aliquot volume of 1  $\mu\text{l}$  for comparison and at the prescribed concentration. Subsequently, the aliquot was combined with a specific volume of the assay buffer solution, leading to a final volume of 200  $\mu\text{l}$ . All samples, inhibitor control solution, and blanks were then gradually added to the enzyme control solution, including NADPH solution (4  $\mu\text{l}$ ), HMG CoA substrate (12  $\mu\text{l}$ ), and HMG CoA reductase (2  $\mu\text{l}$  enzyme). A microplate reader UV/Vis spectrophotometer was used to measure the effectiveness of the sample on HMG CoA enzyme activity at 37 °C  $\lambda=340$  nm and every 10 s for 10 min (Hasim et al., 2018; Sari and Triwahyuni, 2017).

## 2.7. In silico test

Researchers can use the pkcsm tool to analyze a compound's pharmacokinetic properties and obtain the test compound's 3D structure and physicochemical characteristics from Pubchem. Autodock Tools is utilized for preparing test compounds and receptors prior to docking, while Autodock Vina is employed for the docking process and subsequent visualization of the compound through Discovery Studio.

Atorvastatin, simvastatin, gemfibrozil, and nicotinic acid were used to molecularly dock potential chitin compounds to antidiabetic receptor proteins using Autodock 4.2 software, and visualization was carried out using Discovery Studio 2021. Furthermore, the absorption, distribution, metabolism, and excretion of each compound's pharmacokinetic characteristics were predicted using the pkcsm website in <http://biosig.lab.uq.edu.au/pkcsm/prediction>. Hardware specs were then performed on a machine with a core i3, 4 GB of RAM, 64-bit, and 2 GB of nVidia GeForce. The physicochemical characteristics of the selected compounds, including molecular weight, log P, hydrogen donor, and acceptor, were obtained from the PubChem ligand databank in <https://pubchem.ncbi.nlm.nih.gov/>. The crystal structure of the protein

associated with fat mass and obesity that serves as the target receptor was obtained through the RCSB website (pdb: id 3LFM). The most effective conformation out of the 100 compound conformations used for molecular docking was selected for examination of interaction and binding affinity. Molecular dynamics was also carried out to examine the optimum docking outcome (Brogi et al., 2020; Morris et al., 1991). The Gibbs free energy determined through the MMPBSA method and the RMSD graph were the outcomes of the examination of the molecular dynamics data.

## 3. Results

### 3.1. Chitin characterization

Characterization was carried out to ascertain the material to be utilized as well as to identify the proper standards for chitin. Table 1 shows the findings of the mangrove crab shells chitin's characterization.

A reddish-yellow sample from mangrove crab shells was used for the next process. The findings revealed the synthesis of crude chitin after the demineralization process was 34.6 %, indicating relatively low. A chitin crude extract yield of 35.6 % was obtained during the deproteinization procedure. Furthermore, the effectiveness of the process was determined by the amount of NaOH used. The protein in the mangrove crab shell flour dissolved in the base, thereby enabling the separation of the protein that was covalently attached to the chitin functional group. A NaOH solution with a high concentration and temperature was then used to facilitate the separation of the molecules. In this study, the chitin yield was 35.547 %, as shown in Table 1.

Table 2 shows the four metals with the greatest concentrations of chitin in mangrove crab shells, namely calcium (Ca), magnesium (Mg), potassium (K), and phosphate (P). The concept of a hard-soft acid base suggested that chitin, containing an amide and an amine group, can interact strongly with a hard acid, such as magnesium. Furthermore, this makes the removal of Mg very difficult during the demineralization and deproteinization procedures.

Chitin from mangrove crab shells was characterized by functional group identification using FTIR (Fourier Transform Infra Red) and surface morphology with SEM-EDX (Scanning Electron Microscope-Energy Dispersive X-Ray). The mechanism of FTIR testing involved the vibration of atoms within molecules by transmitting electromagnetic waves over the sample to create an infrared spectrum. The proportion in the sample can be identified by focusing on each radiation absorption energy that can be seen at a specific wavelength. The transformation of the extracted mangrove crab shells into chitin can be assessed by comparing the products with the standard compounds.

Based on the comparison of FTIR spectra between chitin from mangrove crab shells and the standard in Table 3 and Fig. 1, the spectrum showed similar wave numbers. Furthermore, each spectrum exhibited the characteristic of chitin compounds. The FTIR analyses indicated the chitin standard spectrum, which featured wave numbers

**Table 1**  
The mangrove crab shells chitin's characterization.

No.	Test Parameters	Values	Standard Value
1	Drying shrink (%)	4.38	Less than 5 %
2	Ethanol soluble level (%)	0.22	Not defined
3	Water soluble level (%)	0.44	Not defined
4	Water content (% v/b)	3.40	Less than 10 %
5	Total ash (% b/b)	70.94	Not defined
6	Acid insoluble ash (% b/b)	64.18	Not defined
7	Extract specific gravity 1 % (g/mL)	1.0233	Not defined
8	Yield (%)	35.547	Not defined
9	Melting point (°C)	289.7	Not defined
10	Total Plate Count (TPC) (cfu/g)	$1.40 \times 10^1$	Less than 105
11	<i>E. coli</i> (cfu/g)	0	Less than 10
12	Mold level (cfu/g)	$1.00 \times 10^1$	Less than 103
13	Yeast level (cfu/g)	0	Less than 103

**Table 2**

Metal content testing and heavy metal contamination of chitin from mangrove crab shells.

No.	Test parameters	Rate (mg/kg)	Standard value (mg/kg)
1	As	<0.0001	5
2	Cd	0.1542	0,3
3	Cu	5.2786	–
4	Hg	<0.0001	0.5
5	K	1041.1891	–
6	Sb	1.6965	–
7	Se	0.1144	–
8	Sn	3.1194	–
9	Bi	<0.0001	–
10	Ca	1767.1493	–
11	Co	0.1642	–
12	Cr	<0.0001	–
13	Fe	79.6020	–
14	Mg	4741.8955	–
15	Pb	3.7114	10
16	Zn	8.6965	–
17	P	12104.9627	–

**Table 3**

Wave number and the functional groups of mangrove crab shells chitin.

No	Vibration type	Wave number region (cm <sup>-1</sup> )	
		Mangrove crab shells chitin	Chitin standard
1	-NH	3448	3436
2	-OH	3273	3268
3	-CH	2931	2886
4	-NH	1658	1661
5	-C-N	1423	1418
6	C-O	1070	1073
7	-NH	1029	1026
8	C-O-C	873	896
9	β-1,4-glycosidic	713	752

for the OH and NH groups, namely 3433 cm<sup>-1</sup>. However, due to the overlap between the absorptions formed by the -NH and OH groups and the wave number 701 cm<sup>-1</sup> for the -1,4-glycosidic group, the 3433 cm<sup>-1</sup> level featured a widespread absorbance (Dompeipen et al., 2016). The chitin from mangrove crab shells was analyzed using SEM-EDX after the functional group test by FTIR to identify the morphological

characteristics. Materials' morphology, surface morphology, and molecular structure can be examined with the SEM-EDX test. SEM has also been used to examine the surface morphology of mangrove crab shells chitin, while EDX was used to determine the elemental composition. Furthermore, mapping has been reported to be used for visualizing the distribution of the elements. The shape of the resultant chitin was then compared to that of a typical variant, as shown in Fig. 2.

The chitin derived from mangrove crab shells (Fig. 3 and Table 4) requires EDX analysis to determine their elemental composition. The percentage of carbon (C) atoms in chitin was 49 %, which was higher compared to O, P, and Ca, as shown in Table 4. Furthermore, C represented purple color was more abundant compared to oxygen (O), phosphorus (P), and calcium (Ca), which were indicated by green, green, and blue coloration, respectively. There was a decrease in the quality of chitin extracted from mangrove crab shells due to the presence of metal content.

### 3.2. Cell viability study of chitin from mangrove crab shells using in vitro MTT assay methods for cytotoxicity testing against HepG2 cells

HepG2 liver cancer cell line was treated in a sufficient culture media to determine the efficacy of chitin in the chemosensitizing ability of chitin, followed by a viability study using MTT assay. The MTT method was carried out by measuring the amount of mitochondrial dehydrogenase in living cell that can convert MTT into formazan, as shown in Fig. 5. Furthermore, the measurement was carried out colorimetrically based on the creation of a purple, insoluble formazan salt from the reduction reaction of tetrazolium, leading to the formation of a water-soluble yellow solution. The presence of live cell was indicated by an intense purple coloration. Results of that inquiry are anticipated to demonstrate the cytotoxic effects of chitin on HepG2 cell, as shown in Fig. 4.

Chitin was tested for its cytotoxicity at concentrations of 1, 25, 50, 75, and 100 µg/mL, as shown in Fig. 4. Based on the assay, it has an IC<sub>50</sub> of 64.39 ± 1.315 µg/mL against HepG2 cell, indicating that it was toxic, as shown in Table 5.

### 3.3. Chitin has a potential effect as an antioxidant agent

A reduction in DPPH absorbance at a wavelength of 515 nm

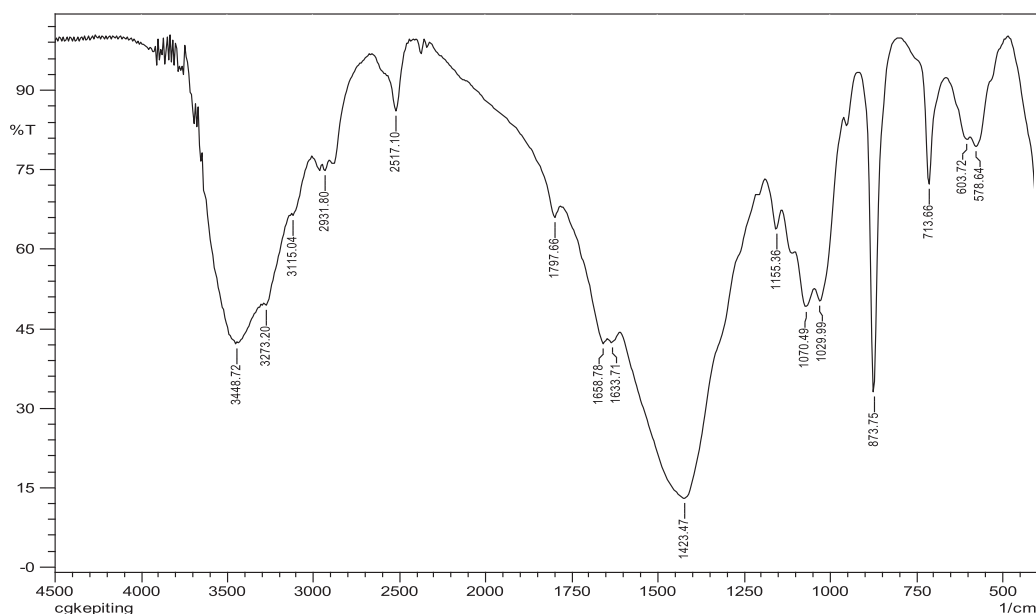


**Fig. 1.** FTIR spectra of chitin from mangrove crab shells.



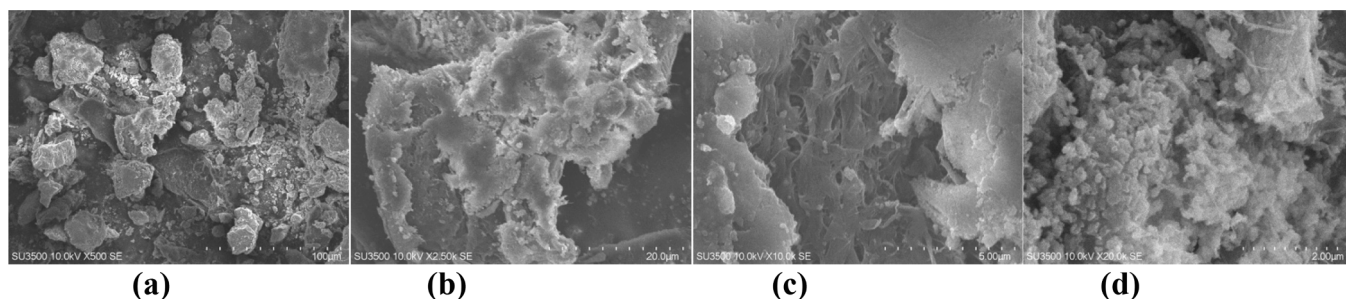


Fig. 2. SEM photographs of chitin from mangrove crab shells with magnification of (a) 100  $\mu\text{m}$ ; (b) 20  $\mu\text{m}$ ; (c) 5  $\mu\text{m}$ ; and (d) 2  $\mu\text{m}$ .

indicated that chitin had an antioxidant activity. Furthermore, antioxidants often interacted with DPPH radicals through proton donation, thereby changing the color from purple to yellow, as shown in Fig. 6.

Chitin's  $\text{IC}_{50}$  value for DPPH inhibition and FRAP method was  $24.38 \pm 0.34 \mu\text{g/mL}$  and  $430 \pm 10.074 \mu\text{g/mL}$  with an AAI value of  $1.62 \pm 0.026$  and  $0.7261 \pm 0.03$ , respectively, as shown in Table 6. These findings indicated that sample had an antioxidant activity. The  $\text{IC}_{50}$  value represented the amount of chitin (in  $\mu\text{g/mL}$ ) required to block the oxidation process by 50%. The greater the antioxidant capacity of a substance, the smaller the  $\text{IC}_{50}$  value. A reference material, namely ascorbic acid was also used to test the antioxidant activity due to its high potency.

Based on the results, ascorbic acid's  $\text{IC}_{50}$  value for DPPH and FRAP was  $0.60 \pm 0.025 \mu\text{g/mL}$  and  $5.35 \pm 0.020 \mu\text{g/mL}$  with AAI value of  $65.66 \pm 1.056$  and  $58.31 \pm 0.056$ , respectively, as shown in Table 6. This indicated that DPPH reduction was an area where ascorbic acid outperformed chitin in terms of antioxidant efficacy. The effectiveness of ascorbic acid was greatly increased due to the presence of a polyhydroxy group. It also possessed a free hydroxy group, which functioned as a free radical scavenger. Ascorbic acid served as a standard in this study. It was also used as a benchmark due to its role as a secondary antioxidant that inhibited extracellular free radicals.

### 3.4. Chitin has a potential effect as an antidiabetic agent

Fig. 8 and Table 7 shows the  $\text{IC}_{50}$  on HMG CoA reductase enzyme for chitin and pravastatin.

Chitin from mangrove crab shells had an  $\text{IC}_{50}$  of  $36.65 \pm 0.082 \mu\text{g/mL}$  and can inhibit the enzyme's activity by up to 68.73% when assayed at a concentration of 100  $\mu\text{g/mL}$ , as shown in Table 7. As a commercial inhibitor, pravastatin was added to the sample, and the results showed that it greatly reduced the enzymatic activity compared to the control enzyme, as shown in Fig. 8. Furthermore, it had an  $\text{IC}_{50}$  of  $6.95 \pm 0.191 \mu\text{g/mL}$  and inhibited the enzyme activity up to 92.82% (Fig. 8 and Table 7), thereby demonstrating the efficiency of the assay system.

### 3.5. Pharmacokinetic, toxicity prediction studies, molecular docking, and dynamics simulations of selected potential compounds of chitin

The analysis of physico-chemical properties is based on Lipinski's law, also known as the rule of five, which states that each value of the rule is a multiple of five. Physico-chemical properties analysis based on structure revealed the number of H donors (NH and OH), H acceptors (N and O), as well as molecular weight, and log P values. According to Lipinski's rule, the H donor requirement is no more than 5, and the H acceptor requirement is no more than 10, which has good permeability. According to Lipinski's rule, the molecular weight of compounds that can penetrate biological membranes based on Lipinski's rule is no more than 500 g/mol; the compound must be molecular, have a small particle size, and be relatively lipophilic. The log P value that satisfies Lipinski's rule is no greater than 5. The log P value describes the ability of the compound to dissolve in biological membrane fluid (octanol/water

solubility).

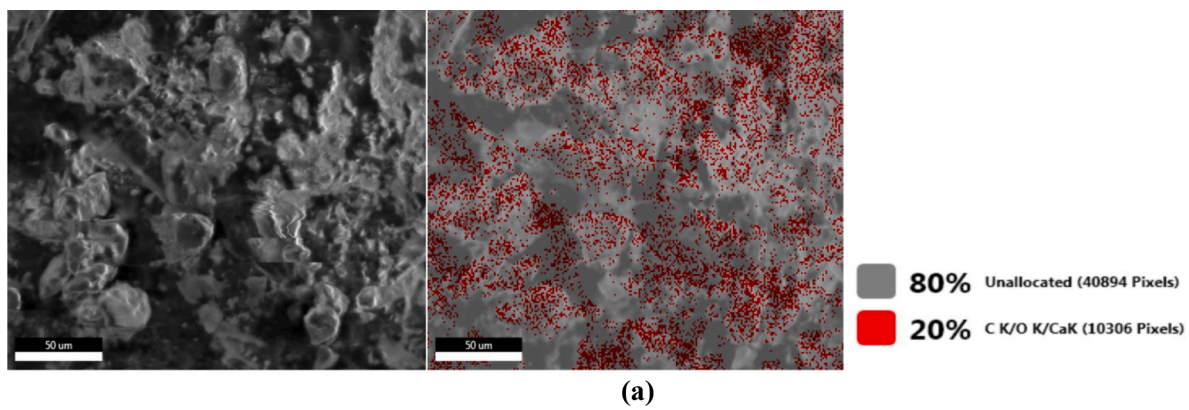
The compounds' physicochemical properties were examined using the structure of the ligands chitin (Fig. 9), molecular weight, and log P (Table 8). Based on the framework, atorvastatin had 4H donors and 3H acceptors, simvastatin had 3H acceptors, gemfibrozil had 1H donor and 3H acceptors, nicotinic acid had 1H donor and 3H acceptors, while chitin had 5H donors and 2H acceptors in the positive control. Furthermore, each ligand had a molecular weight of  $<500 \text{ g/mol}$  with log P values  $< 5$ .

The stability of a three-dimensional structure required the presence of the least intramolecular energy (total steric energy) on the connected atoms and the free electron pair. Therefore, the repulsion force between atoms must be minimized to the lowest levels. The quantity and placement of hydroxyl groups in aromatic rings as well as the unpaired electron have been reported to play a role in the delocalization of electrons. Based on these criteria, atorvastatin, simvastatin, gemfibrozil, nicotinic acid, and chitin met the conditions of the Five Lipinski Rule, indicating that they can be absorbed and distributed in the body. The docking data using AutoDock Vina showed that chitin had the same affinity as the control-positive atorvastatin, simvastatin, gemfibrozil, and nicotinic acid, with an RMSD value of 0.000. This indicated that the selected compounds in the five-star Lipinski Rule parameters were comparable to the positive control. Furthermore, the hydrogen donors and acceptors with a molecular weight of 500 and the acceptor for the hydrogen with a weight of 10, conformed with Lipinski's rule. Based on these criteria, it was projected that the selected potential chitin molecules can be used as medicine.

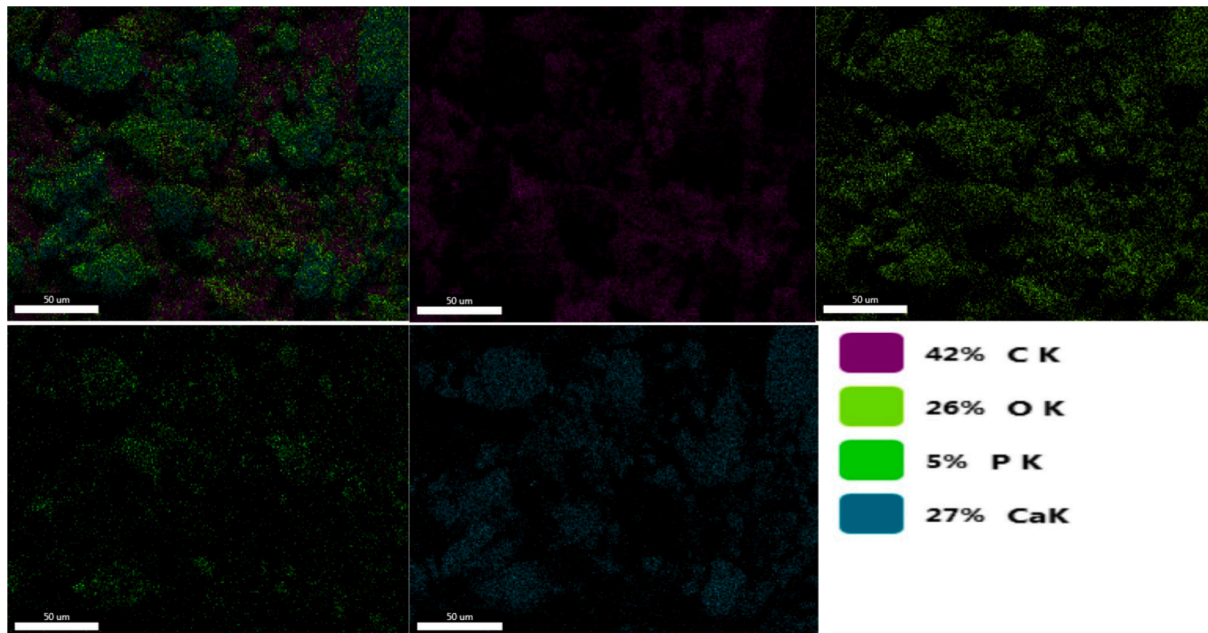
Based on docking studies, all potential chitin ligands showed higher binding affinities compared to nicotinic acid but lower affinities than atorvastatin, simvastatin, gemfibrozil, and the natural ligand. Furthermore, the molecular docking modeling showed that simvastatin, atorvastatin, and gemfibrozil had the greatest binding affinity and inhibition constants with chitin. This indicated that it has a better affinity for the receptor compared to the native ligand. The level of interaction of certain substances with the receptor was indicated by the binding affinity value. Fig. 10 shows the final results of docking visualization by implementing Discovery Studio 2021 on the top-selected compounds from chitin in comparison to the positive control.

Visualization of the docking result of the interaction between chitin and simvastatin, and residues of the binding site water bridges and hydrogen bonds represented the majority of significant ligand-protein interactions identified by the MD simulations, as demonstrated by Fig. 10. Lys 735 and Asp 690 were the two most important amino acids for simvastatin, while Met 657 was the most significant residue in terms of hydrogen bonding for chitin. The important amino acids at HMG CoA reductase receptor are Ser 684, Val 683, and Leu 857. Over the duration of the path, the stacked bar chart is standardized, for instance, a value of 1.0 indicates that a specified interaction was preserved for 100% of the simulation duration. There could be interactions between the ligand and many protein residues. An antidiabetic effect is formed by the bond that is established between these amino acids and subsequent processes.

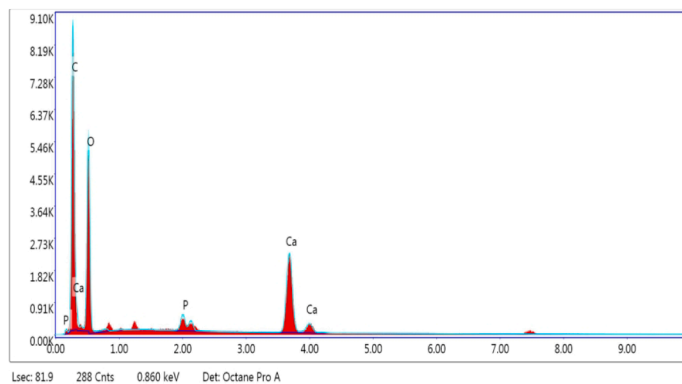
The Root Mean Square Deviation (RMSD) graph showed that chitin,



(a)



(b)



(c)

**Fig. 3.** (a) Mapping analysis EDX images of chitin extracted from mangrove crab shells; (b) Element overlay mapping analysis, CK: Carbon; OK: Oxygen; PK: Phosphorus; and CaK: Calcium; (c) Analysis of EDX of mangrove crab shells chitin; C: Carbon; O: Oxygen; P: Phosphorus; and Ca: Calcium.

simvastatin, and HMG CoA reductase receptor interaction persisted in the binding pocket after a simulation in aqueous condition for 100 ns, as shown in Fig. 10. Furthermore, RMSD was used to analyze the structural activity of both proteins and their complexes. The structural variations based on the interactions between ligands and proteins were fully described by the graph. To assess the stability of the protein complexes,

RMSD plots of the proteins and their complexes were created and compared for the interpretation of the MD simulation results. Compared to the simvastatin chart, establishing that the protein was stabilized after 31.26 ns with an RMSD value of 0.3417, the RMSD chart for the chitin complex originally showed some fluctuation before stabilizing at an RMSD value of 0.2816 after 24.56 ns. This showed that the predicted



**Table 4**  
Analysis of percentage element of EDX of mangrove crab shells chitin.

Element	Weight %	Atomic %
C K (Carbon)	36.61	49.05
O K (Oxygen)	41.96	42.20
P K (Phosphor)	1.24	0.65
CaK (Calcium)	20.18	8.10

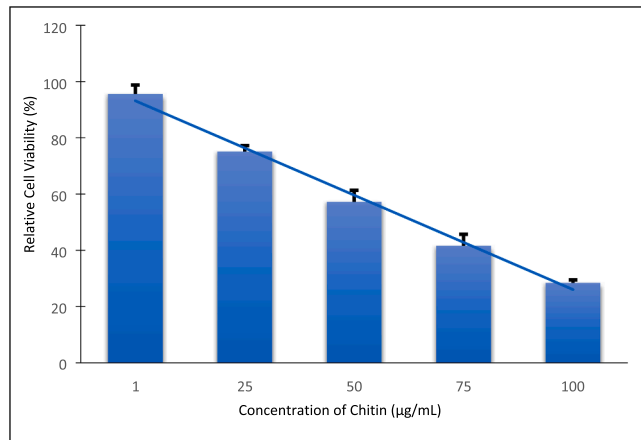


**Fig. 4.** Chitin's effect against HepG2 liver cancer cell appears dose-dependent. Individual HepG2 cell was administered with chitin treatment for 24 h, and the MTT assay was used to determine the vitality of the treated cell.

binding interaction between chitin and HMG CoA reductase receptor was more stable in aqueous conditions compared to simvastatin, which increased docking yield, as shown in Fig. 10 (Hussain et al., 2023; Jarattanachai et al., 2023).

## 4. Discussion

### 4.1. Chitin characterization

The yield of chitin after the demineralization process was relatively low. This can be attributed to the high mineral content, primarily limestone, present in the shell, which prevented the crude chitin from passing through the 80-mesh sieve. Moreover, the use of 1 N HCl solution led to the breakdown and release of minerals, reducing the yield (Jabeen et al., 2023). In this research, the chitin yield was 35.547 %. The

chitin water content of the mangrove crab shells produced was 3.40 %, which satisfied the criterion established by Lesbani, namely a maximum of 10 % to avoid mold damage (Lesbani et al., 2011).

Compared to Lesbani's study, which found 40 % of chitin in mangrove crab shells, the total ash content in this current study was greater. A high ash content was an indication of mineral content, with metal oxide being produced during burning. The quality and level of purity of the generated chitin increased with decreasing ash concentrations. However, the inadequate removal of minerals during the demineralization process caused a high ash content in this study. This was because the washing was not carried out steadily due to the lack of flowing water and stirring (Fadlaoui et al., 2019).

Natural pharmaceutical products must not contain pathogenic microbes, such as *Salmonella* spp., *Staphylococcus aureus*, *Clostridium* spp., *Shigella* spp., and *Pseudomonas aeruginosa*. A total of  $2.4 \times 10^1$  colonies/g was detected during the microbial contamination test, which met the requirement, namely  $<10^4$  cfu/g (Fadlaoui et al., 2019).

Based on the concepts of strong and weak acids, chitin has a ferrous metal (Fe) level of 79.60 mg/kg, which was an intermediate acid. Base does not interact strongly with strong acids, specifically the amides and amines. The bonds were also not readily dissolved by both methods of deproteinization and demineralization. A previous study showed that the metal in chitin cannot be removed totally due to the high iron level in crab shells during the demineralization (Fadlaoui et al., 2019).

As, Cd, Cu, Hg, Sb, Sn, Bi, and Pb are some examples of heavy metal contamination. Furthermore, the presence of copper in the mangrove crab shells indicated that the habitat of crab has been contaminated. A previous study reported that metal concentration significantly decreased throughout the demineralization process (Pandharipande et al., 2016). This was caused by the inability of the amide and amines present in chitosan and chitin to bind to copper, a soft acid.

Chitin has an amorphous solid morphology and a crystalline structure, which typically appeared white. An amorphous solid was often characterized by erratic and unpredictable atomic structure or particle. Furthermore, the most common sources of chitin included shrimp, crab, squid, and lobster. Compared to extracted chitin, the common form appeared rough and clustered, while the typical form was smoother and

**Table 5**

IC<sub>50</sub> on *in vitro* MTT assay methods for cytotoxicity testing against HepG2 cell for chitin.

Sample	IC <sub>50</sub> (µg/mL)
Chitin	64.39 ± 1.315

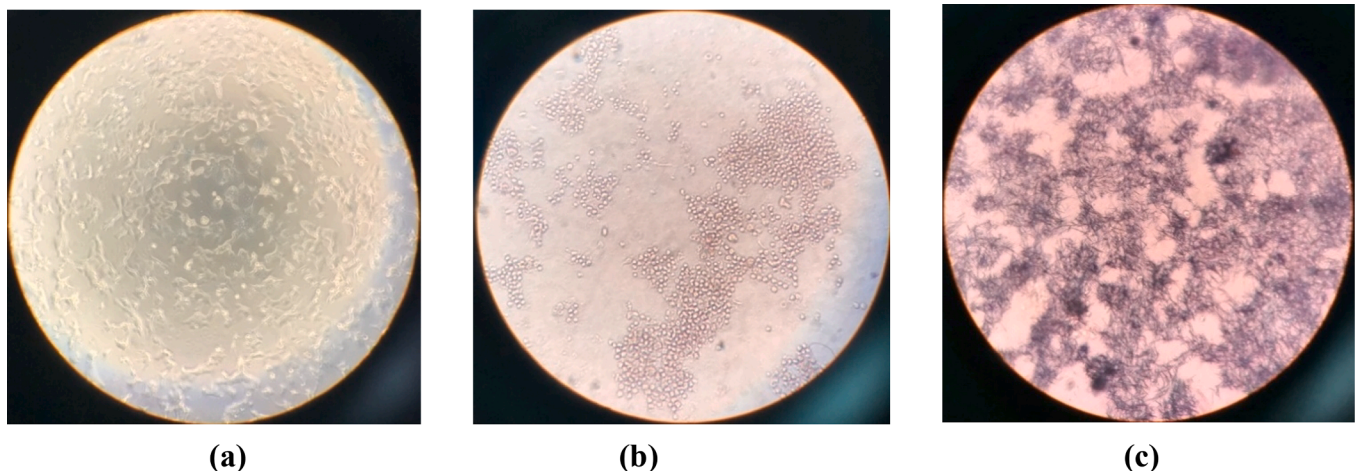


**Fig. 5.** Formazan crystals viewed from a microscope at 400 magnification: (a) cell before MTT treatment; (b) cell after MTT treatment (dead cell); (c) cell after MTT treatment (live cell).

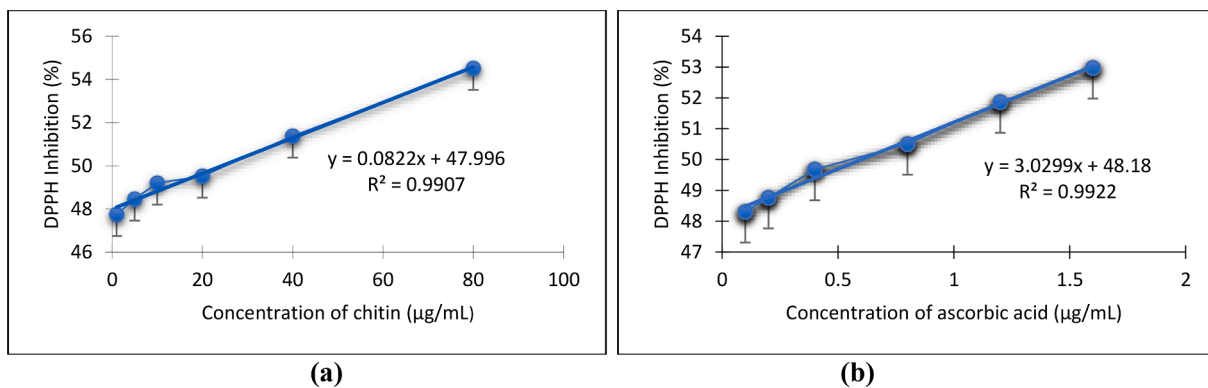


Fig. 6. DPPH radical scavenging activity of (a) chitin; (b) ascorbic acid at various concentrations. The data represent the mean ± SD measurements of samples tested in triplicate.

Table 6

IC<sub>50</sub> values and AAI (Antioxidant Activity Index) of chitin by DPPH and FRAP methods.

Sample	IC <sub>50</sub> DPPH (µg/mL)	AAI DPPH	IC <sub>50</sub> FRAP (µg/mL)	AAI FRAP
Chitin	24.38 ± 0.34	1.62 ± 0.026	430.00 ± 10.074	0.7261 ± 0.03
Ascorbic acid	0.60 ± 0.025	65.66 ± 1.056	5.35 ± 0.020	58.31 ± 0.056

Table 7

IC<sub>50</sub> on HMG CoA reductase activity for chitin and pravastatin.

Sample	IC <sub>50</sub> (µg/mL)
Chitin	36.65 ± 0.082
Pravastatin	6.95 ± 0.191

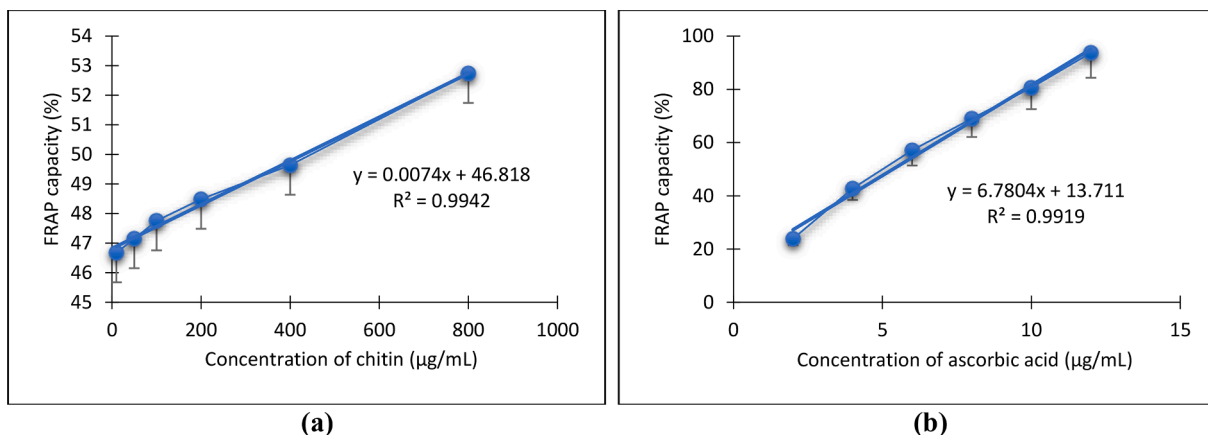


Fig. 7. FRAP capacity of (a) chitin; (b) ascorbic acid in a range of concentrations. The data represent the mean ± SD measurements of samples tested in triplicate.

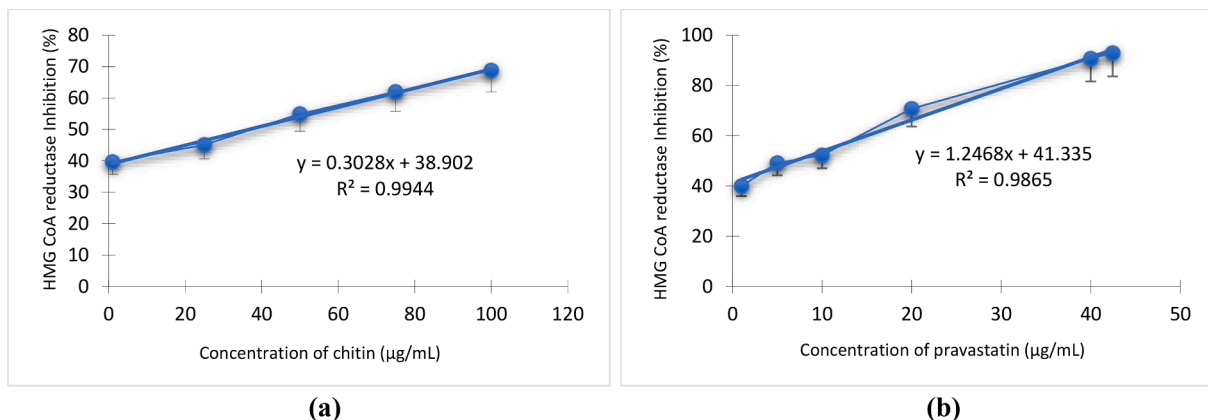


Fig. 8. HMG CoA reductase inhibition on the addition of (a) chitin; (b) pravastatin with several concentrations at 340 nm. The data represent the mean ± SD measurements of samples tested in triplicate.



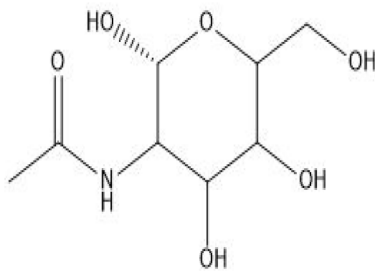


Fig. 9. Chitin ligand structure.

more uniform. This finding indicated that the morphology varied based on the source of the mangrove crabs, and the environment has an impact on the structure (Wahyuni et al., 2020).

Recognizing the final results, the extracted material can further be processed into therapeutic products. The morphology of *Vespa crabro* and *Vespa velutina* had previously been assessed using SEM and characterized as (1) microporous smooth surfaces, (2) fish-scale-shaped nanofibrous surfaces, (3) adhering fibers with nanopores, and (4) divided fibers with nanoholes. These findings are consistent with this study, which obtained similar structures for chitin from mangrove crab

shells. This indicated that carbon (C) had the highest concentration in the samples (Feás et al., 2020).

#### 4.2. Cell viability study of chitin from mangrove crab shells using in vitro MTT assay methods for cytotoxicity testing against HepG2 cells

*In vitro* studies showed that chitin had the potential to sensitize HepG2. The succinate tetrazolium reductase mechanism degraded the MTT reagent through a reduction reaction to produce formazan, which only reacted with still-alive cell (Nair et al., 2020; Nath et al., 2016, 2015).

Chitin was tested for its cytotoxicity at concentrations of 1, 25, 50, 75, and 100  $\mu\text{g}/\text{mL}$ , as shown in Fig. 4. Based on the assay, it has an  $\text{IC}_{50}$  of  $64.39 \pm 1.315 \mu\text{g}/\text{mL}$  against HepG2 cell, indicating that it was toxic, as shown in Table 5. Based on the National Cancer Institute (NCI), the cytotoxic activity of extracts or compounds with  $\text{IC}_{50}$  value of 30  $\mu\text{g}/\text{mL}$ , 30–100  $\mu\text{g}/\text{mL}$ , and >100  $\mu\text{g}/\text{mL}$  were considered active, moderately active, or inactive, respectively. Therefore, it was established that chitin had a moderate level of activity (Nair et al., 2020; Namvaran et al., 2022).

Chitin's cytotoxic activity, antioxidant activity, and antidiarrhea effects have not been previously researched. Methanol extracts of A.

Table 8

Determination of ligands' physicochemical properties, prediction of a pharmacokinetic and predicted molecular toxicity parameter.

Parameters Test	Molecule Name				
	Atorvastatin	Simvastatin	Gemfibrozil	Nicotinic acid	Chitin
<b>Ligands' physicochemical properties</b>					
Log P	5	4.7	3.8	0.4	-2.82
Molecule Weight (g/mol)	558.6	418.6	250.33	123.1	221.21
<b>Absorption parameter at the molecular level</b>					
Intestinal absorption (human) (%Absorbed)	59.861	84.026	94.033	94.099	-1.38
Skin permeability (log Kp)	-2.735	-2.729	-2.701	-2.735	-0.219
Water solubility (logmol/L)	-4.531	-4.529	-3.249	-2.134	31.963
CaCO <sub>2</sub> permeability (log Papp in 10 <sup>-6</sup> cm/s)	0.23	0.421	1.394	1.17	-3.234
P-glycoprotein substrate	Yes	Yes	No	No	No
P-glycoprotein I inhibitor	No	Yes	No	No	No
P-glycoprotein II inhibitor	No	Yes	No	No	No
<b>Distribution parameters of molecules</b>					
VDss (human) (log L/kg)	-1.918	-0.719	-0.541	-1.015	0.041
Fraction unbound (Human)	0.089	0	0.211	0.776	0.856
BBB permeability (log BB)	-1.162	-0.639	0.143	-0.323	-0.618
CNS permeability (log PS)	-2.916	-2.402	-2.380	2.869	-3.694
<b>Metabolism parameters of molecules</b>					
CYP2D6 substrate	No	No	No	No	No
CYP3A4 substrate	Yes	Yes	No	No	No
CYP1A2 inhibitor	No	No	No	No	No
CYP2C19 inhibitor	No	No	No	No	No
CYP2C9 inhibitor	Yes	No	No	No	No
CYP3A4 inhibitor	No	No	No	No	No
<b>Excretion parameters of molecules</b>					
Total clearance (log mL/min/kg)	0.437	-0.083	0.272	0.652	0.711
Renal OCT2 substrate	No	No	No	No	No
<b>Molecular toxicity parameters</b>					
AMES toxicity	No	No	No	No	No
Max. tolerated dose (human) (log mg/kg/day)	0.193	-0.667	0.85	0.907	1.944
hERG I inhibitor	No	No	No	No	No
hERG II inhibitor	No	No	No	No	No
Oral Rat Acute Toxicity (LD50) (mol/kg)	2.877	2.302	2.339	2.24	1.547
Oral Rat Chronic Toxicity (LOAEL) (log mg/kgBW/day)	4.839	0.285	1.953	2.652	3.406
Hepatotoxicity	Yes	No	No	No	No
Skin Sensitisation	No	No	No	No	No
T.Pyri-formis toxicity (log ug/L)	0.285	0.285	0.87	0.055	0.285
Minnow toxicity (log mM)	-0.63	-1.96	0.162	2.222	4.705

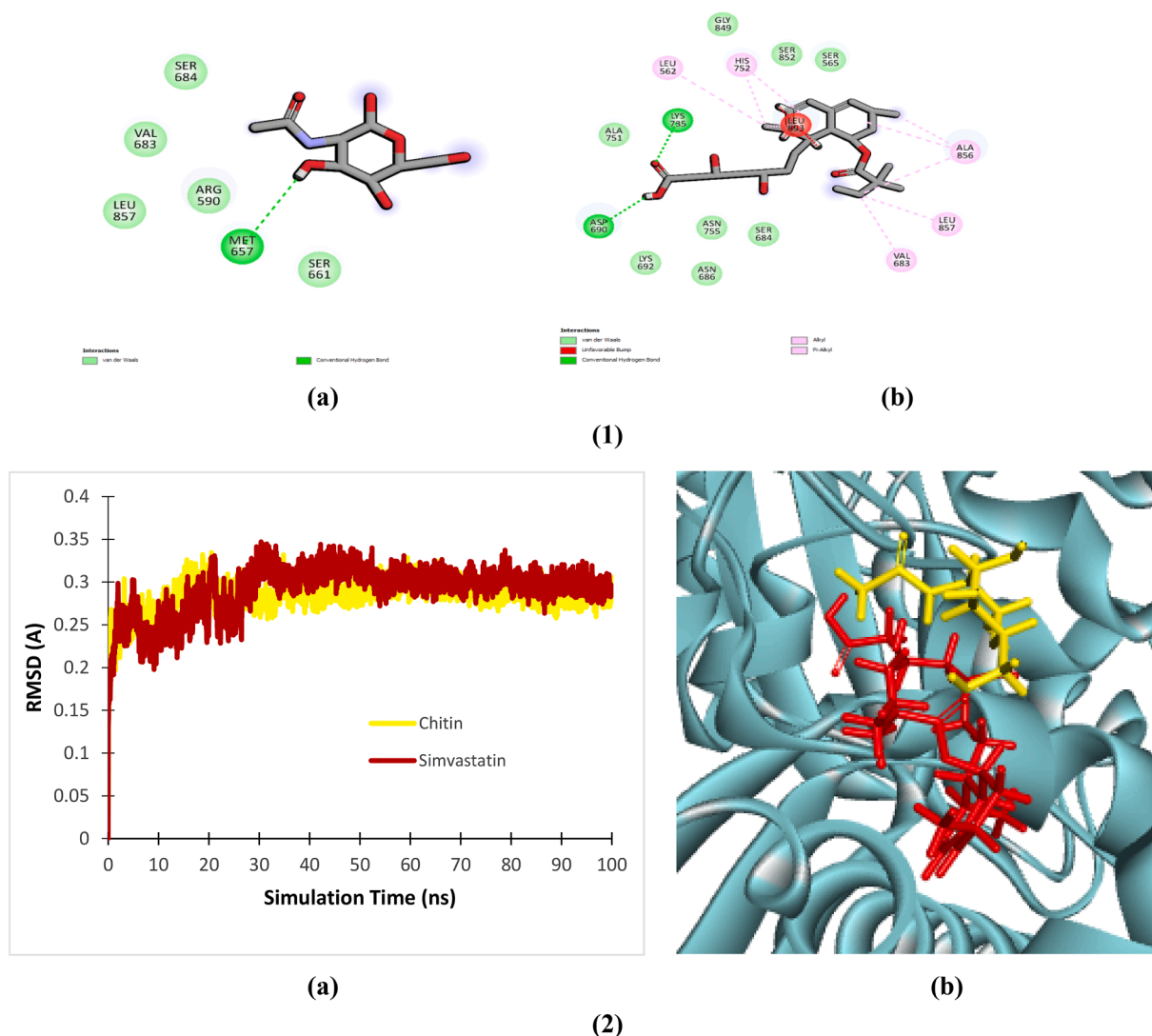


**Fig. 10.** (1) Visualization of the docking result of the interaction between (a) chitin; (b) simvastatin, and residues of the binding site water bridges and hydrogen bonds; (2) (a). Graphic of the root mean square deviation (RMSD) of chitin (yellow) and simvastatin (red) with HMG CoA reductase molecular dynamics were executed for 100 ns duration modeling techniques with the addition of different variables according to the actual physique conditions, including temperature specified as 310 K and a quantity of solvents.

cobbe leaves and *M. longiflora* barks have been shown to have antioxidant activity and cytotoxicity against HepG2 cells. These extracts have strong cytotoxic effects on HepG2 cells, with  $IC_{50}$  values ranging from 11.3  $\mu\text{g}/\text{mL}$  to 54.42  $\mu\text{g}/\text{mL}$ . Compared to other substances, chitin has about the same level of activity as extract of hexane, dichloromethane, and ethyl acetate from *S. castaneifolia* leaves. *Castaneifolias* exhibited considerable cytotoxicity with an  $IC_{50}$  value of 60  $\mu\text{g}/\text{mL}$  against HepG2 cells following 48 h of incubation. Other investigations have demonstrated that *Carallia brachiata* leaf and peel extract exhibits less or inactive cytotoxicity towards HepG2 cells ( $IC_{50} > 100 \mu\text{g}/\text{mL}$ ) while displaying potent antioxidant properties (Namvaran et al., 2022).

Reactive oxygen radicals were compounds with a significant influence on the occurrence of carcinogenesis, including the appearance of liver cancer. This indicated that the toxic effect was due to the presence of antioxidant compounds, which contributed to reducing the number of HepG2 cell. These findings are consistent with previous studies that chitin had moderate antioxidant activity (Goh et al., 2022).

#### 4.3. Chitin has a potential effect as an antioxidant agent

Chitin's  $IC_{50}$  value for DPPH inhibition and FRAP method was 24.38

$\pm 0.34 \mu\text{g}/\text{mL}$  and  $430 \pm 10.074 \mu\text{g}/\text{mL}$  with an AAI value of  $1.62 \pm 0.026$  and  $0.7261 \pm 0.03$ , respectively, and ascorbic acid's  $IC_{50}$  value for DPPH and FRAP was  $0.60 \pm 0.025 \mu\text{g}/\text{mL}$  and  $5.35 \pm 0.020 \mu\text{g}/\text{mL}$  with AAI value of  $65.66 \pm 1.056$  and  $58.31 \pm 0.056$ , respectively as shown in Table 6.

Based on a reduction reaction between a yellow  $\text{Fe}^{3+}$  complex product (potassium hexacyanoferrate) and a bluish-green  $\text{Fe}^{2+}$  complex and that donates electrons in an acidic solution, the FRAP equipment was created. The FRAP test method can be monitored by detecting the  $\text{Fe}^{2+}$  complex's absorbance using a UV-Vis spectrophotometer at a maximum wavelength of 700 nm (Fig. 7) (Cele et al., 2022). The FRAP antioxidant test was relatively rapid, allowing for speedy findings.

The categorization of antioxidants was determined based on the AAI, where values of 0.5,  $> 0.5-1$ ,  $> 1-2$ , and  $> 2$  were classified as weak, moderate, strong, and very strong, respectively. Therefore, ascorbic acid had a strong antioxidant activity, while chitin was in the moderate category with AAI of  $> 2$  and  $> 0.5-1$ , respectively. Considering the one-way ANOVA with a post-hoc Tukey-Kramer multiple comparative teste, the effect of chitin was not significantly different from that of ascorbic acid. This was because it can act as an antioxidant when the OH group was substituted (González-Burgos and Gómez-Serranillos, 2021).

In the DPPH antioxidant method, chitin contributed protons and transformed into a radical compound when it interacts with free radicals. Antioxidants often interacted with DPPH radicals through the mechanism of proton donation. The presence of concentrated unpaired electrons led to the formation of the chitin radical compound, which has very low energy and was significantly less reactive, thereby increasing the ability to suppress DPPH free radicals (Goh et al., 2022).

A previous study showed antioxidant activity under acid conditions in the FRAP test often decreased due to acid protonation (Cele et al., 2022). The ability of chitin to decrease  $\text{Fe}^{3+}$  at pH 6.6 diminished because the electrons in the ionized oxygen atom were more effectively stabilized compared to those in ascorbic acid. Furthermore, the electrons were stabilized by conjugating with the unsaturated carbonyl system and forming an intramolecular hydrogen bond (1,6) with the proton of the aliphatic hydroxy group in the ascorbic acid (Karuna et al., 2018).

The scavenging mechanism of chitin and chitosan was suggested by Trang Si Trung and Huynh Nguyen Duy Bao, where nitrogen's action on chitin's C-2 location produced a free radical-scavenging activity. This was because the nitrogen in amino groups had a single pair of electrons, and can acquire an ammonium ( $\text{NH}_3^+$ ) group when the proton has been released from an acidic solution. A stable molecule can be formed after the reaction of free radicals with the  $\text{NH}_3^+$  hydrogen ion (Si Trung and Bao, 2015).

#### 4.4. Chitin has a potential effect as an antidiyslipidemic agent

HMG CoA reductase was a key enzyme for controlling metabolism and cholesterol synthesis in the liver. Therefore, inhibition of its activity had become a therapeutic target for lowering cholesterol synthesis. Chitin from mangrove crab shells had an  $\text{IC}_{50}$  of  $36.65 \pm 0.082 \mu\text{g/mL}$  and can inhibit the enzyme's activity by up to 68.73 % when assayed at a concentration of  $100 \mu\text{g/mL}$ , as shown in Table 7. It also caused HMG CoA reductase to behave as an inhibitory agent. Furthermore, the inhibition of the enzyme by chitin led to a decrease in the production of mevalonate from HMG CoA decreased. To reduce the intake of exogenous cholesterol, chitin was often bound to cholesterol in the duodenal and jejunal lumen (Baskaran et al., 2015; Sari and Triwahyuni, 2017).

The primary treatment for dyslipidemic diseases used in this study as a comparator was pravastatin. The results showed that its usage for the inhibition of 3-hydroxy-3-methylglutaryl-CoA reductase's (HMG CoA reductase) activity was effective in treating hyperlipidemia with notable outcomes. The mechanism of action of pravastatin involved the inhibition of cholesterol production. Sterol regulatory element-binding proteins (SREBPs) were subsequently degraded on the membrane by proteases and transferred to the nucleus as a result (Pangestika et al., 2020).

As a commercial inhibitor, pravastatin was added to the sample, and the results showed that it greatly reduced the enzymatic activity compared to the control enzyme, as shown in Fig. 8. Furthermore, it had an  $\text{IC}_{50}$  of  $6.95 \pm 0.191 \mu\text{g/mL}$  and inhibited the enzyme activity up to 92.82 % (Fig. 8 and Table 7), thereby demonstrating the efficiency of the assay system. Patients with hypercholesterolemia have experienced a reduction in cholesterol levels of 20–30 % after the use of pravastatin, a mevastatin derivative that was classified as the same as lovastatin. After the treatment and prevention of cardiovascular disease among hypercholesterolemia patients, statin group compounds were frequently employed (Miyajima et al., 2022). Based on the results, it was assumed that chitin can inhibit enzyme activity but was less effective compared to pravastatin.

At present, there are no studies on the effectiveness of chitin as an HMG CoA inhibitor. However, chitosan and its derivatives were formed from its deacetylation and contained N-acetylglucosamine units. In several studies, N-acetylglucosamine has been used as a replacement therapy for managing metabolic syndrome. The application of chitosan has been shown to reduce total cholesterol (TC) and low-density lipoprotein (LDL-C) cholesterol levels in the plasma. A previous study also

reported that it became more viscous during cationization ( $-\text{NH}$ ) and the formation of polycations and gels form. Dietary fiber can lower blood cholesterol in individuals with high intestinal viscosity by inhibiting bile acid metabolism, delaying micelle formation, reducing the rate of cholesterol absorption in the intestine, and inhibiting the diffusion from micelles to the mucosa. Chitosan has also been reported to have strong anti-dyslipidemic activity and played a role in lowering the risk of coronary disease caused by a high-fat diet (Ahn et al., 2021; Yan et al., 2020).

This current study found a significant correlation (Pearson product-moment test) between HMG CoA reductase inhibition, DPPH radical scavenging activity, and FRAP capacity of chitin, with coefficients of determination of 0.97 and 0.97, respectively. A value approach of +1 was also obtained, which represented a perfectly positive correlation. A positive  $r$  value indicated a positive correlation between DPPH radical scavenging activity and HMG CoA reductase, as well as between these two enzymes and chitin's FRAP capacity. Based on these findings, the antioxidant activity of chitin tended to increase along with HMG CoA reductase. The main mechanism of chitin's antidiyslipidemic effect against the enzyme's inhibition was based on radical scavenging and FRAP capacity.

#### 4.5. Pharmacokinetic, toxicity prediction studies, molecular docking, and dynamics simulations of selected potential compounds of chitin

As shown in Table 8, each selected compound's pharmacokinetic and toxicity (Table 8) characteristics were based on *in silico* predictions. These results allow for the conclusion that all compounds can bind to HMG CoA reductase receptor with an adsorption percentage of >90 %, except chitin, with  $\geq 30$  % (Dong et al., 2018; El fadili et al., 2022). Furthermore, chitin has an adsorption percentage of over  $-1.38$  % because it has a water solubility of 31.963. Based on the AMES test results, none of the chemicals were projected to be mutagens, and atorvastatin was potentially hepatotoxic (Table 8), (Dong et al., 2018; Hussain et al., 2023) indicating that further *in vitro* and *in vivo* tests were required (Raies and Bajic, 2016; Rim, 2020). The examination of physicochemical attributes showed that chitin compounds have high permeability. The docking results also revealed the compounds can bind to HMG CoA reductase, HMG synthase, LDL receptor, PPAR-alpha, and HCAR-2 receptors, leading to the formation of antidiyslipidemic effects (Brogi et al., 2020). Table 9 shows the docking outcomes for the selected substances at antidiyslipidemic receptors using Autodock 4.2 (Dong et al., 2018; Morris et al., 1991; Raies and Bajic, 2016).

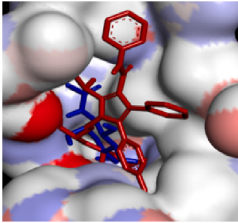
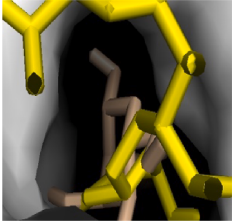
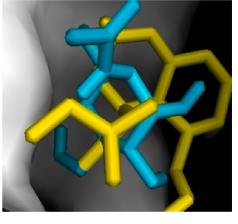
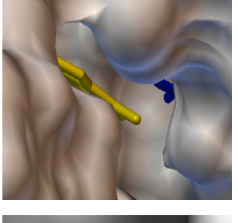
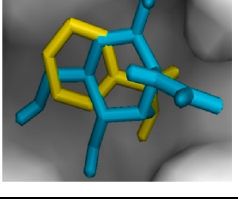
The Van der Waals effect was a molecular mechanics component that contributed to the electrostatic component in the Poisson-Boltzmann-calculated solvation-free energy. This energy was derived from a nonpolar contribution using an empirical model, and the delta-G binding-free energy was calculated using the total balance of all components, as shown in Table 10. Furthermore, the free energy calculation was based on the size of the Poisson-Boltzmann Surface (MMPBSA) and referred to the results of molecular dynamics. Based on the comparison between simvastatin and chitin compounds, simvastatin generally had lower delta G. This was because its nonpolar group had more contribution compared to that of chitin, which was similarly nonpolar. Another causal factor was simvastatin's tendency to be more lipophilic in terms of chemical structure. Simvastatin had a free energy of  $-82.071 \text{ kcal/mol}$ , while chitin has a free energy of  $-26.341 \text{ kcal/mol}$ . This suggested that chitin was predicted to have a moderately stable binding affinity with HMG CoA reductase receptors (Akhmadiev et al., 2019; Alizadeh et al., 2022).

## 5. Conclusions

Based on the results, *in-vitro* antioxidant and antidiyslipidemic analysis revealed that chitin from mangrove crab shells has powerful antioxidant activity in the DPPH radical scavenging method and

**Table 9**

The outcome of molecular docking of selected chitin compounds to antidyslipidemic receptors.

Receptor	Molecule Name	Affinity (kcal/mol)	Number of Hydrogen Bonds	Active Site Cavity	The Amino Acid Residue Involved
HMG Co-A Reductase	Atorvastatin	-9.5	3		Lys691, Asp690, Lys692, Ser684, Arg590,
	Chitin	-5.7	5		
HMG Synthase	Simvastatin	-6.9	1		Asn135, Leu270, Asn343, Thr171, Ala168, Gly218, Val216
	Chitin	-5.8	3		
Receptor LDL	Simvastatin	-4.6	1		Arg162, Phe132, Gln133, Asn135, Gln161
	Chitin	-3.6	1		
PPAR-Alpha	Gemfibrozil	-6.	1		Ile272, Cys275, Cys276, Met330, Ile339
	Chitin	-5.6	2		
HCAR 2	Nicotinic acid	-3.7	2		Ser98, Val97, Lys94, Glu38, Asn54, Leu52, Ser53
	Chitin	-4.6	5		

**Table 10**

The effect of chitin and simvastatin on HMG CoA reductase molecular dynamics.

Energy component contribution	Chitin (kcal/mol)	Simvastatin (kcal/mol)
Van der Waal energy	-99.595 ± 28.752	-161.156 ± 17.064
Electrostatic energy	-62.329 ± 27.595	-92.018 ± 14.485
Polar solvation energy	147.486 ± 44.960	188.816 ± 24.633
SASA energy	-11.903 ± 2.124	-17.713 ± 0.853
SAV energy	0.000 ± 0.000	0.000 ± 0.000
WCA energy	0.000 ± 0.000	0.000 ± 0.000
Binding energy	-26.341 ± 19.325	-82.071 ± 19.915

moderate effects in the FRAP method compared to ascorbic acid. It has also been reported to have HMG CoA reductase inhibitory, lipid-lowering, and moderately cytotoxic activities in HepG2 cell. Furthermore, chitin from mangrove crab shells has a good affinity for HMG CoA

reductase, HMG synthase, LDL, PPAR-alpha, and HCAR-2 receptors compared to native ligands and positive controls. This indicated that it can be considered a candidate for anti-dyslipidemia drugs. The predicted binding interaction between chitin and HMG CoA reductase receptor was more stable in aqueous conditions. According to Lipinski's rule, they also have drug-likeness compared to positive controls, with an estimated absorption rate in the intestinal system of >90 %. However, more detailed and comprehensive preclinical and clinical studies are needed to establish the lipid-lowering and antidyslipidemia efficacy of chitin.

#### CRediT authorship contribution statement

The experiment was conceptualized by Inarah Fajriaty, I Ketut Adnyana, Irda Fidrianny, and Neng Fisher Kurniati and Inarah Fajriaty planned, organized, and carried out the experiment as well as the computational experiment; evaluated and interpreted the results; prepared the manuscript. The paper was revised by Nosyahida Mohd Fauzi and Sarmila Hanim Mustafa. The final, published version of the paper



has been read and approved by all authors. All authors have read and agreed to the published version of the manuscript.

### Declaration of competing interest

The authors declare that they have no known competing financial interests or personal relationships that could have appeared to influence the work reported in this paper.

### Acknowledgments

The authors are grateful for the funding provided through the Sandwich Program of World Class University Funding, Institut Teknologi Bandung, as well as the Education (LPDP) Grant of the Indonesia Endowment Fund.

### Appendix A. Supplementary data

Supplementary data to this article can be found online at <https://doi.org/10.1016/j.sjbs.2024.103964>.

### References

- Ahn, S.I., Cho, S., Choi, N.J., 2021. Effectiveness of chitosan as a dietary supplement in lowering cholesterol in murine models: a meta-analysis. *Mar. Drugs*. <https://doi.org/10.3390/MD19010026>.
- Akhmadiev, N.S., Galimova, A.M., Akhmetova, V.R., Khairullina, V.R., Galimova, R.A., Agletdinov, E.F., Ibragimov, A.G., Kataev, V.A., 2019. Molecular docking and preclinical study of five-membered S, S-palladadeterocycle as hepatoprotective agent. *Adv. Pharm. Bull.* 9, 674–684. <https://doi.org/10.15171/apb.2019.079>.
- Aklog, Y.F., Egusa, M., Kaminaka, H., Izawa, H., Morimoto, M., Saimoto, H., Ifuku, S., 2016. Protein/CaCo3/Chitin nanofiber complex prepared from crab shells by simple mechanical treatment and its effect on plant growth. *Int. J. Mol. Sci.* 17 <https://doi.org/10.3390/ijms17101600>.
- Al-Abbad, E., Alakhras, F., 2020. Removal of dye acid red 1 from aqueous solutions using chitosan-iso-vanillin sorbent material. *Indonesian. J. Sci. Technol.* 5, 352–365. <https://doi.org/10.17509/ijost.v5i3.24986>.
- Alizadeh, A.A., Jafari, B., Dastmalchi, S., 2022. Drug Repurposing for Identification of S1P1 agonists with Potential Application in Multiple Sclerosis Using in Silico Drug Design Approaches. *Adv. Pharm. Bull.* 10.34172/apb.2023.012.
- Baskaran, G., Salvamani, S., Ahmad, S.A., Shaharuddin, N.A., Pattiram, P.D., Shukor, M. Y., 2015. HMG-CoA reductase inhibitory activity and phytochemical investigation of *Basella alba* leaf extract as a treatment for hypercholesterolemia. *Drug Des. Devel. Ther.* 9, 509–517. <https://doi.org/10.2147/DDDT.S75056>.
- Broggi, S., Ramalho, T.C., Kuca, K., Medina-Franco, J.L., Valko, M., 2020. Editorial: in silico methods for drug design and discovery. *Front. Chem.* <https://doi.org/10.3389/fchem.2020.00612>.
- Budiana, W., Suhardiman, A., Roni, A., Sumarah, I., Nara, T.E., 2017. Antioxidant activity of leaf extracts of three genera *Artemisia* sp by DPPH method and determination of total flavonoid, phenol and carotenoid levels. *Kartika: Jurnal Ilmiah Farmasi* 5, 38. <https://doi.org/10.26874/kjif.v5i2.106>.
- Cele, N., Awolade, P., Seboletswe, P., Olofinson, K., Islam, M.S., Singh, P., 2022.  $\alpha$ -Glucosidase and  $\alpha$ -Amylase Inhibitory Potentials of Quinoline-1,3,4-oxadiazole Conjugates Bearing 1,2,3-Triazole with Antioxidant Activity, Kinetic Studies, and Computational Validation. *Pharmaceuticals* 15, 1035. <https://doi.org/10.3390/ph15081035>.
- Daniar, A.V., Herdyastuti, N., 2019. The Effect Of Chitin Size And Soaking Time On Decreasing Cholesterol Levels On Quail Eggs.
- Domeipen, E.J., Kaimudin, M., Dewa Balai Riset dan Standarisasi Industri Ambon, R.P., Cengkeh, J., Merah Ambon, B., 2016. Isolation of chitin and chitosan from waste of skin shrimp.
- Dong, J., Wang, N.N., Yao, Z.J., Zhang, L., Cheng, Y., Ouyang, D., Lu, A.P., Cao, D.S., 2018. Admetlab: A platform for systematic ADMET evaluation based on a comprehensively collected ADMET database. *J. Cheminform* 10. <https://doi.org/10.1186/s13321-018-0283-x>.
- El Fadili, M., Er-Rajy, M., Kara, M., Assougum, A., Belhassan, A., Alotaibi, A., Mrabti, N. N., Fidan, H., Ullah, R., Ercisli, S., Zarougui, S., Elhallaoui, M., 2022. QSAR, ADMET In Silico Pharmacokinetics, Molecular Docking and Molecular Dynamics Studies of Novel Bicyclo (Aryl Methyl) Benzamides as Potent GlyT1 Inhibitors for the Treatment of Schizophrenia. *Pharmaceuticals* 15, 670. <https://doi.org/10.3390/ph15060670>.
- Fadlaoui, S., El Asri, O., Mohammed, L., Sihame, A., Omari, A., Melhaoui, M., 2019. Isolation and characterization of chitin from shells of the freshwater crab *potamon algeriense*. *Prog. Chem. Appl. Chitin Deriv* 24, 23–35. <https://doi.org/10.15259/PCACD.24.002>.
- Feás, X., Vázquez-Tato, M.P., Seijas, J.A., Nikalje, A.P.G., Fraga-López, F., 2020. Extraction and Physicochemical Characterization of Chitin Derived from the Asian Hornet, *Vespa velutina* Lepeletier 1836 (Hym.: Vespidae). *Molecules* 25. Doi: 10.3390/molecules25020384.
- Goh, M.P.Y., Kamaluddin, A.F., Tan, T.J.L., Yasin, H., Taha, H., Jama, A., Ahmad, N., 2022. An evaluation of the phytochemical composition, antioxidant and cytotoxicity of the leaves of *Litsea elliptica* Blume – an ethnomedicinal plant from Brunei Darussalam. *Saudi J. Biol. Sci.* 29, 304–317. <https://doi.org/10.1016/j.sjbs.2021.08.097>.
- González-Burgos, E., Gómez-Serranillos, M.P., 2021. Effect of phenolic compounds on human health. *Nutrients*. <https://doi.org/10.3390/nu13113922>.
- Hasim, H., Hasanah, Q., Andrianto, D., Nur Faridah, D., 2018. Antioxidant And Antihypercholesterolemia Activities In Vitro From Mixture Of Rumber And Branch Extract. *Jurnal Teknologi Dan Industri Pangan* 29, 145–154. <https://doi.org/10.6066/jtip.2018.29.2.145>.
- Hazqil Kadzim, M., Hartati, E., 2020. Recovery of chitin from crab shell waste. *Serambi Engineering*.
- Hussain, A., Hussain, A., Sabnam, N., Kumar Verma, C., Shrivastava, N., 2023. In silico exploration of the potential inhibitory activity of DrugBank compounds against CDK7 kinase using structure-based virtual screening, molecular docking, and dynamics simulation approach. *Arab. J. Chem.* 16 <https://doi.org/10.1016/j.arabjc.2022.104460>.
- Imtihani, H.N., Permatasari, S.N., Prasetya, R.A., 2021. In Vitro Evaluation of Cholesterol-Reducing Ability of Chitosan from Mangrove Crab (*Scylla serrata*) Shell Solid Dispersion using PVP K-30 as a Carrier. *Jurnal Farmasi Galenika (Galenika Journal of Pharmacy) (e-Journal)* 7, 99–109. <https://doi.org/10.22487/j24428744.2021.v7.i2.15597>.
- Islam, M.K., Ha, S., Baek, A.-R., Yang, B.-W., Kim, Y.-H., Park, H.-J., Kim, M., Nam, S.-W., Lee, G.-H., Chang, Y., 2022. The Synthesis, Characterization, Molecular Docking and In Vitro Antitumor Activity of Benzothiazole Aniline (BTA) Conjugated Metal-Salen Complexes as Non-Platinum Chemotherapeutic Agents. *Pharmaceuticals* 15, 751. <https://doi.org/10.3390/ph15060751>.
- Jabeen, F., Younis, T., Sidra, S., Muneer, B., Nasreen, Z., Saleh, F., Mumtaz, S., Saeed, R. F., Abbas, A.S., 2023. Extraction of chitin from edible crab shells of *Callinectes sapidus* and comparison with market purchased chitin. *Braz. J. Biol.* 83 <https://doi.org/10.1590/1519-6984.246520>.
- Jarerattanachai, V., Boonarkart, C., Hannongbua, S., Auwarakul, P., Ardkhean, R., 2023. In silico and in vitro studies of potential inhibitors against Dengue viral protein NS5 Methyl Transferase from Ginseng and Notoginseng. *J. Tradit. Complement. Med.* 13, 1–10. <https://doi.org/10.1016/j.jtcm.2022.12.002>.
- Karuna, D.S., Dey, P., Das, S., Kundu, A., Bhakta, T., 2018. In vitro antioxidant activities of root extract of *Asparagus racemosus* Linn. *J. Tradit. Complement. Med.* 8, 60–65. <https://doi.org/10.1016/j.jtcm.2017.02.004>.
- Kidibule, P.E., Santos-Moriano, P., Plou, F.J., Fernández-Lobato, M., 2020. Endo-chitinase Chit33 specificity on different chitinolytic materials allows the production of unexplored chitoooligosaccharides with antioxidant activity. *Biotechnol. Rep.* 27. <https://doi.org/10.1016/j.btre.2020.e00500>.
- Kong, C.S., Kim, J.A., Bak, S.S., Byun, H.G., Kim, S.K., 2011. Anti-obesity effect of carboxymethyl chitin by AMPK and aquaporin-7 pathways in 3T3-L1 adipocytes. *J. Nutr. Biochem.* 22, 276–281. <https://doi.org/10.1016/j.jnutbio.2010.02.005>.
- Lesbani, A., Yusuf, S., Melviana, R.A., 2011. Chitin and Chitosan Characterization from Mangrove Crab Shell (*Scylla Serrata*). *Jurnal Penelitian Sains* 14 (3C).
- Maesaroh, K., Kurnia, D., Al Anshori, J., 2018. Comparison of Antioxidant Activity Test Methods of DPPH, FRAP and FIC Against Ascorbic Acid, Gallic Acid and Quercetin. *Chemica Et Natura Acta* 6, 93. <https://doi.org/10.24198/cna.v6.n2.19049>.
- Miyajima, C., Hayakawa, Y., Inoue, Y., Nagasaka, M., Hayashi, H., 2022. HMG-CoA Reductase Inhibitor Statins Activate the Transcriptional Activity of p53 by Regulating the Expression of TAZ. *Pharmaceuticals* 15, 1015. <https://doi.org/10.3390/ph15081015>.
- Morris, G.M., Goodsell, D.S., Pique, M.E., Huey, R., Forli, S., Hart, W.E., Halliday, S., Bewle, R., Olson, A.J., 1991. User Guide AutoDock Version 4.2 Updated for version 4.2.6 Automated Docking of Flexible Ligands to Flexible Receptors.
- Nair, B., Anto, R.J., Sabitha, M., Nath, L.R., 2020. Kaempferol-mediated sensitization enhances chemotherapeutic efficacy of sorafenib against hepatocellular carcinoma: an in silico and in vitro approach. *Adv. Pharm. Bull.* 10, 472–476. <https://doi.org/10.34172/apb.2020.058>.
- Namvaran, A., Fazeli, M., Farajnia, S., Hamidian, G., Rezazadeh, H., 2022. Effects of *Scrophularia oxyssepala* Methanolic Extract on Early Stages of Dimethylhydrazine-Induced Colon Carcinoma in Rats: Apoptosis Pathway Approach. *Adv. Pharm. Bull.* 12, 835–841. <https://doi.org/10.34172/apb.2022.085>.
- Nath, L.R., Gorantla, J.N., Joseph, S.M., Antony, J., Thankachan, S., Menon, D.B., Sankar, S., Lankalappalli, R.S., Anto, R.J., 2015. Kaempferide, the most active among the four flavonoids isolated and characterized from *Chromolaena odorata*, induces apoptosis in cervical cancer cells while being pharmacologically safe. *RSC Adv.* 5, 100912–100922. <https://doi.org/10.1039/c5ra19199h>.
- Nath, L.R., Gorantla, J.N., Thulasidasan, A.K.T., Vijayakurup, V., Shah, S., Anwer, S., Joseph, S.M., Antony, J., Veena, K.S., Sundaram, S., Marelli, U.K., Lankalappalli, R.S., Anto, R.J., 2016. Evaluation of uttroside B, a saponin from *Solanum nigrum* Linn, as a promising chemotherapeutic agent against hepatocellular carcinoma. *Sci. Rep.* 6 <https://doi.org/10.1038/srep36318>.
- Ongtanapat, T., Prommee, N., Jampa, O., Limcharoen, T., Wanmasae, S., Nissapatorn, V., Paul, A.K., Pereira, M. de L., Wilairatana, P., Nasongkla, N., Eawsakul, K., 2022. The Cholesterol-Modulating Effect of the New Herbal Medicinal Recipe from Yellow Vine (*Coscinium fenestratum* (Goettg.)), Ginger (*Zingiber officinale* Roscoe.), and Safflower (*Carthamus tinctorius* L.) on Suppressing PCSK9 Expression to Upregulate LDLR Expression in HepG2 Cells. *Plants* 11. <https://doi.org/10.3390/plants11141835>.
- Pandharipande, S.L., Bhagat, P.H., Professor, A., Tech, B., Semester, T.H., 2016. Synthesis of Chitin from Crab Shells and its Utilization in Preparation of Nanostructured Film. *Int. J. Sci. Eng. Technol. Res. (IJSETR)* 5.

- Pangestika, I., Oksal, E., Tengku Muhammad, T.S., Amir, H., Syamsimir, D.F., Wahid, M. E.A., Andriani, Y., 2020. Inhibitory effects of tangeretin and trans-ethyl caffeate on the HMG-CoA reductase activity: potential agents for reducing cholesterol levels. *Saudi J. Biol. Sci.* 27, 1947–1960. <https://doi.org/10.1016/j.sjbs.2020.06.010>.
- Payyappallimana, U., Venkatasubramanian, P., 2016. Exploring ayurvedic knowledge on food and health for providing innovative solutions to contemporary healthcare. *Front. Public Health* 4, 57. <https://doi.org/10.3389/fpubh.2016.00057>.
- Raies, A.B., Bajic, V.B., 2016. In silico toxicology: computational methods for the prediction of chemical toxicity. *Wiley Interdiscip. Rev.: Comput. Mol. Sci.* 147–172 <https://doi.org/10.1002/wcms.1240>.
- Rim, K.T., 2020. In silico prediction of toxicity and its applications for chemicals at work. *Toxicol. Environ. Health. Sci.* <https://doi.org/10.1007/s13530-020-00056-4>.
- Sari, R., Triwahyuni, W., 2017. HMG-KoA Reduktase (Exploration of Medicinal Forest Plants with HMG-CoA Reductase Inhibitory Activity).
- Shebis, Y., Iluz, D., Kinel-Tahan, Y., Dubinsky, Z., Yehoshua, Y., 2013. Natural Antioxidants: Function and Sources. *Food Nutr. Sci.* 04, 643–649. <https://doi.org/10.4236/fns.2013.46083>.
- Si Trung, T., Bao, H.N.D., 2015. Physicochemical properties and antioxidant activity of chitin and chitosan prepared from Pacific White Shrimp Waste. *Int. J. Carbohydrate Chem.* 2015, 1–6. <https://doi.org/10.1155/2015/706259>.
- Wahyuni, S., Selvina, R., Fauziyah, R., Prakoso, H.T., Priyono, P., Siswanto, S., 2020. Optimization of Temperature and Time of Chitin Deacetylation in Maggot Cells (*Hermetia ilucens*) to Produce Chitosan). *Jurnal Ilmu Pertanian Indonesia* 25, 373–381. <https://doi.org/10.18343/jipi.25.3.373>.
- Wittriansyah, K., Handayani, M., Dirgantara, D., 2018. Characterization Of Chitin And Chitosan Emerita Sp. From Widarapayung Coast, Cilacap, Central Java. *Jurnal Ilmiah Samudra Akuatika* 2, 45–51.
- Wulansari, D., Chairul, D., Botani, B., Penelitian, P., Abstrak, B.-L., 2011. Antioxidant screening activity of several Indonesian medicinal plants using 2,2-difenil 1–1 picrylhidrazyl (DPPH). *Majalah Obat Tradisional*.
- Yan, C., Zhang, C., Cao, X., Feng, B., Li, X., 2020. Intestinal Population in Host with Metabolic Syndrome during Administration of Chitosan and Its Derivatives. *Molecules.* <https://doi.org/10.3390/MOLECULES25245857>.
- Yunarto, N., Aini, N., Oktoberia, I.S., Sulistyowati, I., Kurniatri, A.A., 2019. Antioxidant Activity and Inhibition of HMG CoA and Lipase from the Combination of Binahong-Temu Lawak Leaf Extract. *Jurnal Kefarmasian Indonesia* 89–96. <https://doi.org/10.22435/jki.v9i2.1930>.

### Further Reading

- Benet, L.Z., Hosey, C.M., Ursu, O., Oprea, T.I., 2016. BDDCS, the Rule of 5 and drugability. *Adv. Drug Deliv. Rev.* <https://doi.org/10.1016/j.addr.2016.05.007>.